JOURNAL OF GEOPHYSICAL RESEARCH, VOL. 104, NO. D1, PAGES 1645–1661, JANUARY 20, 1999

# Nitric acid and ammonia at a rural northeastern U.S. site

B. L. Lefer[1] and R. W. Talbot

Institute for the Study of Earth, Oceans, and Space, and Earth Sciences Department, University of New Hampshire
Durham

J. W. Munger

Department of Earth and Planetary Sciences, Harvard University, Cambridge, Massachusetts

**Abstract.** Hourly mixing ratios of $HNO_3$, $NH_3$ and various other trace gas and aerosol species were determined at Harvard Forest in central Massachusetts between 1991 and 1995 in order (1) to ascertain the representativeness of this composite data set, (2) to identify general seasonal and diurnal trends in the mixing ratios of $HNO_3$ and $NH_3$ at this site, (3) to establish how these mixing ratios depend on characteristic meteorological parameters such as wind direction and temperature, and (4) to examine $HNO_3$ relative to the other reactive nitrogen species measured. Harvard Forest receives air masses from both urban and rural source regions resulting in mean midday $HNO_3$ mixing ratios 4 times higher when surface winds were from the SW (~ 2000 parts per trillion by volume (pptv)) as opposed to the NW (~ 500 pptv) wind sector. The $HNO_3$ diel cycle provides evidence of entrainment of $HNO_3$ from aloft as the nocturnal inversion breaks down. Gaseous $NH_3$ mixing ratios are typically 200-300 pptv and on average exhibit little diel variability. High levels of atmospheric sulfate consistently suppress $NH_3$ concentrations below the predicted $NH_3$ compensation point of the canopy, even during periods when the sum of $NH_3$ and $NH_4^+$ ($NH_X$) mixing ratios are quite high. The aerosol $SO_4^{2-}$ regulation of $NH_X$ partitioning changes as a function of temperature. At the same $SO_4^{2-}$ mixing ratio, colder ambient temperatures result in lower $NH_3/NH_X$. On average $HNO_3$ makes up about 20% of $NO_Y$ at midday. The sum of the measured $NO_Y$ species (NO, $NO_2$, $HNO_3$, and particulate $NO_3^-$) typically account for 60-80% of $NO_Y$, suggesting that peroxyacetylnitrate and other organic nitrates are a significant fraction of $NO_Y$ at this predominantly oak forested site.

## 1. Introduction

The family of odd nitrogen trace species known as $NO_Y$ ($NO_Y \equiv NO + NO_2 + NO_3 + N_2O_5$ + nitric acid ($HNO_3$) + aerosol nitrate ($NO_3^-{}_{(p)}$) + peroxyacetylnitrate (PAN) + other organonitrates) is integral to the chemistry of the atmosphere. Besides regulating the rate of ozone ($O_3$) production and destruction reaction sequences, NO and $NO_2$ also affect tropospheric mixing ratios of hydroxyl (OH) and hydroperoxy ($HO_2$) radicals. By controlling these critical atmospheric oxidants, $NO_X$ (NO + $NO_2$) is effectively involved in most atmospheric reaction cycles and the $NO_X$ mixing ratio controls oxidative removal rates of many trace gases.

$NO_X$ is directly emitted from combustion processes as NO but rapidly reacts with various oxidants (e.g., $O_3$, $HO_2$, organic peroxy radicals ($RO_2$)) to form $NO_2$. In the presence of sunlight, the photodissociation of $NO_2$ can regenerate NO in a matter of minutes, while slower reactions, occurring over a period of hours to days, may further oxidize $NO_2$ to nitric acid ($HNO_3$) or peroxyacetylnitrate (PAN). At night, $NO_2$ can be oxidized (via $O_3$) to $NO_3$ or subsequently react with $NO_3$ to form $N_2O_5$, that hydrolyses on aerosol surfaces to produce $HNO_3$ [*Richards*, 1983; *Dentener and Crutzen*, 1993].

The less reactive $NO_Y$ reservoir species (PAN and $HNO_3$) have different atmospheric fates. PAN is only stable at cold temperatures and essentially insoluble, and as such has the potential to be transported long distances in the cold upper troposphere. Thus delivered to remote regions, PAN can thermally decompose to $NO_X$ in subsiding air. Although $HNO_3$ can react with various gases and particles (e.g., ammonia ($NH_3$) and soil/dust particles) to form nitrate containing aerosols, it is also very water soluble and readily adsorbs onto surfaces. Due to the large deposition velocity of $HNO_3$ it is efficiently removed from the atmosphere via both wet and dry deposition processes over short transport distances. Given the slow removal mechanisms of the other $NO_Y$ components, the removal of $HNO_3$ is the primary atmospheric $NO_Y$ sink.

Further interest in the fate of $HNO_3$ has been linked to the "fertilization" of N-limited ecosystems by atmospheric deposition [*Schindler and Bayley*, 1993]. As anthropogenic emissions of NO have steadily increased over the past several decades [*Gschwandtner et al.*, 1986], so has the deposition of atmospheric nitrogen [*Schell*, 1987], thereby potentially inducing some systems to incorporate even more atmospheric $CO_2$ [*Peterson and Melillo*, 1985]. These investigations have highlighted the shortage of information regarding boundary layer $HNO_3$ mixing ratios and deposition fluxes, largely due to the difficulty in obtaining reliable ambient measurements. Even more scarce, and probably more difficult to acquire, are

---

[1] Now at Advanced Study Program, NCAR, Boulder, Colorado.

Paper number 1998JD100016.
0148-0227/99/1998JD100016$09.00

accurate measurements of gaseous $NH_3$ [*Williams et al.*, 1992], another potentially important source of N to the biosphere.

In addition to being an important nutrient for plant growth, $NH_3$ is the only gaseous base found in significant quantities in the atmosphere, and it is therefore fundamental in determining the overall acidity of cloudwater, precipitation, and atmospheric aerosols. Important sources of $NH_3$ include the decay of domestic livestock wastes, volatilization losses from fertilizers, biomass burning, and senescing vegetation [*Schlesinger and Hartley*, 1992]. Several studies indicate that growing vegetation can passively absorb or emit $NH_3$ directly through leaf stomata [*Denmead et al.*, 1976; *Farquhar et al.*, 1980; *Langford and Fehsenfeld*, 1992]. When ambient $NH_3$ mixing ratios are below a certain "compensation point," determined by the partial pressure of $NH_3$ within leaf stomata and perhaps the physiological state of the plant, $NH_3$ can escape to the atmosphere. The stomatal uptake of $NH_3$ is essentially the reverse process. *Farquhar et al.* [1980] noted that the compensation point of snap beans (*Phaseolus vulgaris*) was temperature dependent and could be described as the equilibrium $NH_3$ vapor pressure above an ammonium solution at a fixed *p*H of 6.8 (estimated to be the *p*H of the stomatal cell walls) and a $NH_4^+$ concentration of 46 μM. *Langford and Fehsenfeld* [1992] observed a nearly identical relationship for the regulation of background $NH_3$ mixing ratios for air passing over the Roosevelt National Forest in Colorado and suggested that the $NH_3$ compensation point was a non-species specific mechanism perhaps related to photorespiration and assimilation.

Once $NH_3$ is released to the atmosphere, it has an average tropospheric lifetime of the order of hours to days before either (1) reacting with $H_2SO_4$ or $HNO_3$ to form a fine aerosol, (2) being scavenged by wet deposition, or (3) directly dry depositing to the Earth's surface. While $NH_4^+$ may be involved in long-range transport if vertically advected into the free troposphere, $NH_3$ is typically deposited near its source.

Automated instruments to continuously measure atmospheric levels of $NH_3$ [*Wyers et al.*, 1993] and $HNO_3$ [*Buhr et al.*, 1995] have only recently been developed, consequently few long-term or high-resolution data sets exist for either species. The available longer term $NH_3$ measurements (weekly sample integration) indicate a seasonal cycle with summertime maxima and wintertime minima for the Harvard Forest in Petersham, Massachusetts [*Tjepkema et al.*, 1981]. Higher resolution (2 hour integration) summertime data show similar diurnal trends with nighttime minima and daytime maxima for $NH_3$ [*Langford et al.*, 1992]. It is thought the season and diel cycles of $NH_3$ arise from warmer temperatures leading to greater $NH_3$ emission rates.

Several years of weekly $HNO_3$ measurements reveal different trends for various regions of the United States. [*Meyers et al.*, 1991]. Variable $HNO_3$ seasonal trends may be a consequence of episodic $HNO_3$ events occurring throughout the year [*Edgerton et al.*, 1992]. The typical $HNO_3$ diel signal of higher values midday and lower levels at night [*Parrish et al.*, 1986] is thought to be a result of photochemical $HNO_3$ production and surface deposition [*Kleinman et al.*, 1994].

In the present study hourly measurements of $HNO_3$ and $NH_3$ have been obtained during 1991-1995 at a nonurban continental site for a wide range of meteorological conditions. Over the same period, NO, $NO_X$, $NO_Y$ and other important trace gas species and meteorological parameters were continuously measured [*Munger et al.*, 1996, 1998]. The purposes of this study were (1) to ascertain the representativeness of this composite data set, (2) to identify general seasonal and diurnal trends in the mixing ratios of $HNO_3$ and $NH_3$ at this site, (3) to establish how these mixing ratios depend on characteristic meteorological parameters such as wind direction and temperature, and (4) to examine $HNO_3$ relative to the other reactive nitrogen species measured.

## 2. Methods

### 2.1. Site Description and Ancillary Measurements

The Harvard Forest in Petersham (42°32' N, 72°11' W; elevation 340 m) is located in a wooded, rural area of central Massachusetts. The nearest large cities are Boston and Hartford, 100 km to the east and southwest, respectively. This 50-70 year old predominantly oak forest (mixed with maple, beech, birch, cherry, spruce, and pine) has an average canopy height of 23 m near the sampling site. Since the middle of 1990, the Harvard group has made continuous measurements of various atmospheric trace gases (NO, $NO_2$, $NO_Y$, CO, $CO_2$, $H_2O$, $O_3$, and a suite of nonmethane hydrocarbons) from the top of a 30 m tower [*Goldstein et al.*, 1995; *Goulden et al.*, 1996; *Munger et al.*, 1996]. In addition, numerous micrometeorological and radiative properties (including wind speed, wind direction, temperature, relative humidity, photosynthetically active radiation, solar albedo, and net radiative flux) are continuously monitored by a variety instruments collaboratively operated by both Harvard and the State University of New York at Albany [*Moore et al.*, 1996]. The fast response nature of most of these sensors enables the eddy covariance determination of fluxes of heat, momentum, $NO_Y$, $CO_2$, and $O_3$ [*Wofsy et al.*, 1993; *Goulden et al.*, 1996; *Moore et al.*, 1996; *Munger et al.*, 1996, 1998].

### 2.2. Gas Sampling Methods and Protocols

Water soluble gases were sampled with a mist chamber, also known as a nebulizing-reflux chamber [*Cofer et al.*, 1985; *Talbot et al.*, 1990]. A mist chamber concentrates the water soluble gases from a large volume (~1000 L) of air into a small volume (~ 15 mL) of stripping solution, in this case, ultrapure water was used. The dissolved ions in the stripping solution were quantified by ion chromatography. The mist chamber/ion chromatography (MC/IC) method has been continually developed and improved over the past 10 years and has proven in various intercomparison studies to be very effective at sampling gaseous $HNO_3$, HCOOH, $CH_3COOH$, and $SO_2$ [*Keene et al.*, 1989; *Talbot et al.*, 1990; *Stecher et al.*, 1997].

A Teflon membrane (Zefluor™, Gelman Products Inc.) is used as an aerosol prefilter to prevent water soluble aerosols from being dissolved in the mist chamber stripping solution. A custom-made Teflon filter holder, designed to minimize internal surface area by omitting any backup filter support, attaches directly to the glass inlet of the mist chamber sampler [*Klemm and Talbot*, 1991]. Operating at a flow rate of 30 standard liters per minute (slpm), this downward-facing prefilter collects a bulk sample of aerosol particles with a diameter between ~ 10 nm (J. Dibb and B. Anderson, personal communication, 1996) and at least 50 μm for wind speeds up to 5 m $s^{-1}$ [*Davies*, 1968; *Davies and Subari*, 1982]. Aerosol filter samples were stored in a freezer and within a week of

**Table 1.** Mist Chamber $HNO_3$ and $NH_3$ Sampling Dates

| Year | Julian Day |
|---|---|
| 1991 | 165*, 166*, 168, 169*, 223*, 225*, 226*, 227*, |
| 1992 | 143, 144, 146, 147, 148, 192, 193, 194, 245, 246, 248, 249 |
| 1993 | 62, 79, 80, 81, 118, 119, 121, 200*, 201*, 202*, 203*, 204* |
| 1994 | 144*, 153*, 154*, 155*, 156*, 161*, 162*, 167*, 168*, 215*, 216*, 217*, 202*, 235*, 236*, 237*, 238* |
| 1995 | 116*, 117*, 120*, 122*, 159*, 160*, 161*, 164*, 165*, 166*, 167*, 168*, 169*, 213*, 214*, 215*, 219*, 220*, 221* |

$HNO_3$ data collected on all days.
* $NH_3$ data only collected on these dates.

their collection were treated with 200 μL of MeOH (to allow more complete wetting of Teflon) and then extracted with two 10 mL aliquots of deionized water. Immediately after their generation, mist chamber samples and aerosol extracts were stored in 30 mL high density polyethylene amber bottles, preserved with 100 μL of $CHCl_3$ and kept on ice until their transfer to a refrigerator. All samples were analyzed within 2 months of collection by ion chromatography for major ion species (including $NO_3^-$ and $NH_4^+{}_{(aq)}$). Details of the ion chromatography chemical analysis of water soluble gas and aerosol samples are described by *Talbot et al.* [1992, 1997] and *Lefer et al.* [1994].

The hourly sampling protocol involved collecting 45-50 min integrated mist chamber and aerosol prefilter samples simultaneously from three levels (29, 24, and 11 m above ground) with the remaining 10-15 min available to rinse the mist chambers, to change the prefilters, and to periodically collect mist chamber blanks. Unless otherwise noted, this paper will discuss the gas and aerosol samples collected from the uppermost sampling height at 29 m, some 6-7 m above the canopy. Hourly mist chamber samples were continuously collected for 12-30 hour long periods on 70 dates between 1991 and 1995 (Table 1). The majority of the sampling occurred during the growing season (May - August). The entire Harvard Forest data set, including the University of New Hampshire (UNH) gas and aerosol data, is available on-line via anonymous ftp at io.harvard.edu and the Web site www-as.harvard.edu.

### 2.3. Potential Sampling Artifacts

Any $HNO_3$ or $NH_3$ measurement technique that employs a prefilter is susceptible to certain positive and negative artifacts [*Appel and Tokiwa*, 1981; *Cadle et al.*, 1982]. The easiest way to minimize prefilter reactions is to sample for a shorter period of time (smaller volume of air), thereby reducing the aerosol loading on the Teflon prefilter. Our 45 min integrated samples (1.3 $m^3$) were relatively short considering that most studies which observed prefilter problems (see below) typically sampled for 6-24 hours integrating much larger volumes of air (5-20 $m^3$).

On a Teflon filter, particulate $NH_4NO_3$ can volatilize into $HNO_3$ and $NH_3$ [*Appel et al.*, 1981] resulting in significant positive $HNO_3$ [*Spicer et al.*, 1982; *Appel et al.*, 1988] and $NH_3$ [*Appel et al.*, 1988] errors. While $NH_4NO_3$ is volatile at typical tropospheric temperatures and relative humidities [*Stelson and Seinfeld*, 1982], the reactions producing ammonium (bi)sulfate are generally thought to be irreversible [*Tang*, 1980]. High levels of acidic sulfate in the eastern United States probably has the effect of reducing atmospheric $NH_3$ concentrations, by forming involatile ammonium sulfate particles, to values below that required for solid $NH_4NO_3$ to form. The studies that observed positive $HNO_3$ and $NH_3$ artifacts occurred in the western United States where $NH_4NO_3$ is more prevalent due to lower regional $SO_2$ emissions [*Hidy*, 1978; *Wolff*, 1984]. The substantial $SO_4^{2-}$ wet deposition flux to the northeastern United States [*National Atmospheric Deposition Program*, 1997] indicates that $NH_4NO_3$ volatilization should be less of problem when sampling this generally sulfate rich acidic atmosphere.

A potential negative $HNO_3$ artifact can occur when $HNO_3$ reacts with basic soil [*Forrest et al.*, 1982] or sea-salt particles [*Savoie and Prospero*, 1982] on the prefilter. As suggested above, the northeastern United States aerosol is generally acidic, although this acidity can be mitigated by high soil dust emissions occurring as a result of drought or agricultural practices. Aerosol $Ca^{2+}$ (an indicator of soil dust) and $Na^+$ levels on the prefilter were measured for each sample. During this study the mean (± standard deviation) mixing ratios of particulate $Ca^{2+}$ and $Na^+$ were measured to be 75±89 ($n$=371) and 287±370 ($n$=425) pptv, respectively [*Lefer*, 1997]. While there is no straightforward way to correct gaseous $HNO_3$ measurements for prefilter reactions with basic particles, 24 $HNO_3$ samples collected during periods with $Na^+$ mixing ratios more than three standard deviations from their mean (i.e., > 1395 pptv) were excluded from the data set. Nine of these 24 high $Na^+$ samples were collected on the same day during a rare peroid of strong easterly winds. It was assumed that the measured loadings of aerosol $Ca^{2+}$ were insufficient to cause a sampling artifact.

Finally, an acidic prefilter will not affect the sampling of acid gases (e.g., $HNO_3$); however, acidic aerosols could react with $NH_3$ in the sample airstream. Preliminary lab tests indicate that the relatively low aerosol loading in the 45-50 min sample is not sufficient to be a serious issue. Nevertheless, when trying to measure low levels of $NH_3$, a prefilter can easily cause problems. No correction to the $NH_3$ data has been applied for this potential negative artifact.

### 2.4. Mist Chamber Technical Specifications

This MC/IC gas sampling system had average detection limits of 5 pptv for $HNO_3$ and 12-40 pptv $NH_3$, assuming an average solution volume of 15 mL, an average sampled air volume of 1350 L, analytical detection limits (in μmol/L) of 0.02 ($NO_3^-$) and 0.05 ($NH_4^+$), and/or a minimum $NH_4^+$ concentration of 2 times the average blank of 0.09 μmol/L. While the mist chambers did not have a detectable $NO_3^-$ blank, in some cases there was a slight $NH_4^+$ blank associated with the interior mist chamber glass surface that tended to decrease over the course of both single and multiday sampling periods. Since blanks were collected several times a day, this was easily accounted for in the blank correction protocol.

The mist chamber samplers have a shown on multiple occasions to have 100% collection efficiency for $HNO_3$ [*Talbot et al.*, 1990, 1997]. A single-stage $NH_3$ dilution system was constructed to determine the mist chamber's collection effi-

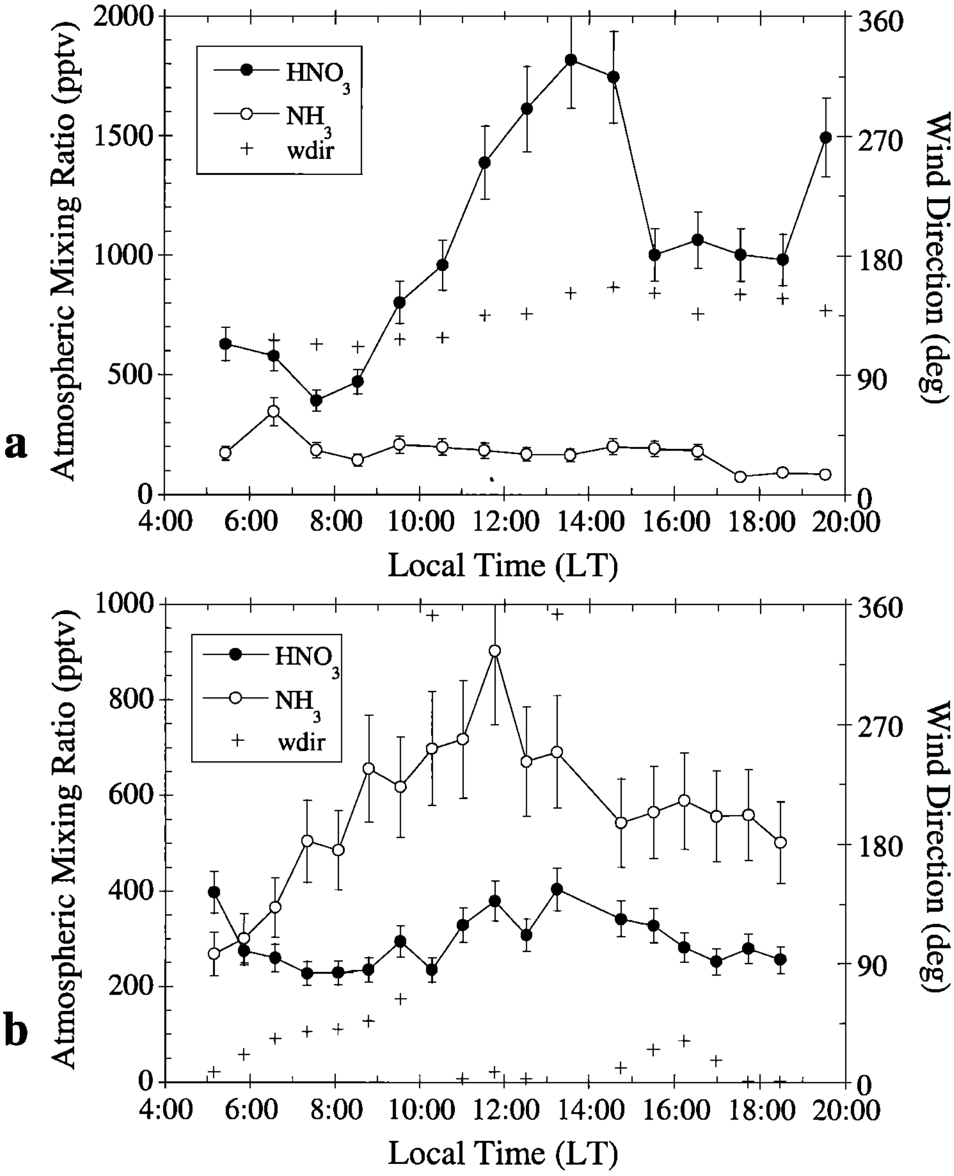

**Figure 1.** (a) Hourly integrated mixing ratios of $HNO_3$ and $NH_3$ and average wind direction for August 3, 1995 (J.D. 215). Error bars represent measurement uncertainty. [b] Same as Figure 1a, but for June 14, 1995 (J.D. 165).

ciency for $NH_3$. This simple dilution system consisted of (1) a $NH_3/N_2$ cylinder (~ 1 ppmv) as calibration source, (2) a high-pressure liquid $N_2$ dewar as a source of diluent gas, (3) two Teledyne-Hastings flowmeters to measure $N_2$ and $NH_3$ flows, and (4) a 1.1 m long 2.0 cm ID Pyrex tube sampling manifold with 3.1 mm add port and a 6.35 mm sample port (near opposite ends). The flow rate of the $NH_3$ cylinder was not measured during an actual calibration run; however, this flow rate was measured before and after each calibration run and always found to be invariant. The concentrated $NH_3$ was transported via a 1 m length of 1/8" OD Silcosteel™ tubing (Restek Inc.) and added into the core of the $N_2$ flow. The flow rate and volume of the dilution $N_2$ was measured by an integrating mass flowmeter upstream from the glass manifold. Approximately 1 m downstream from the $NH_3$ add port, the $NH_3/N_2$ mixture was sampled directly from the core of the manifold with a mist chamber.

The $NH_3$ mixing ratio delivered from the cylinder (821±40 ppbv) was determined by sampling (*n*=12) directly from the Silcosteel™ tubing. The cylinder gas was bubbled through 2 $H_2O$ bubblers in series followed by a mass flowmeter. No $NH_4^+$ was ever detected in the second bubbler. For a typical ambient $NH_3$ mixing ratio (370 pptv), the mist chamber had a mean (± standard deviation) collection efficiency of 99% (±9.2%) (*n*=9). Similar $NH_3$ collection efficiencies were observed for both higher and lower $NH_3$ levels. A mist chamber collection efficiency of 100% was used for determining the mixing ratios of both $HNO_3$ and $NH_3$ in our ambient air measurements.

The uncertainties assigned to the atmospheric mixing ratios reported for MC/IC samples were calculated using the error propagation formula [*Knoll*, 1979] and applying it to the uncertainties associated with the following measurements: air volume, water volume, ion concentration, blank subtraction,

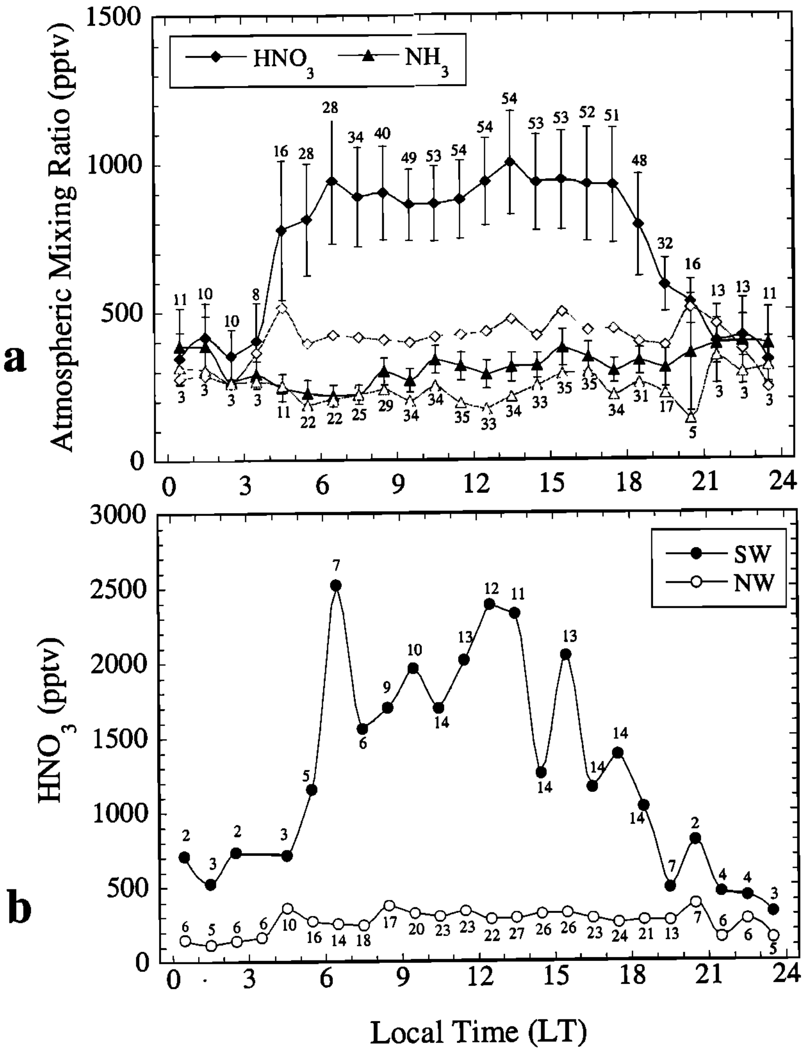

Figure 2. (a) Mean (solid symbols) and median (open symbols) summertime diel cycles of $HNO_3$ (diamonds) and $NH_3$ (triangles) for all wind sectors. Error bars represent standard error of mean. Numbers above or below bars are number of hourly samples averaged. (b) Median $HNO_3$ diel cycles for the dominant wind sectors: 180°-270° is southwest (SW) and 270°-45° is northwest (NW). Values above or below points are number of samples.

and collection efficiency. The reported mixing ratios of $HNO_3$ and $NH_3$ have overall uncertainties of ±11% and ±18%, respectively. The accuracy of the ion chromatographic determinations of $NO_3^-$ and $NH_4^+$ in mist chamber samples were referenced to National Institute of Standards and Technology certified aqueous standards; however, at this point there are no certified low-level (sub-ppbv) gaseous standards to directly determine the overall accuracy of any measurement of these and many other trace gases [*Crosley*, 1994].

## 3. Results

### 3.1. Diel Cycles of $HNO_3$ and $NH_3$

Changes in mixing ratios of both species were often related to changes in wind direction or the height of the mixed layer, day 215 of 1995 (Figure 1a) is a good example of "typical" diurnal behavior at this site because of consistent winds from the south-southeast throughout the day. Under these conditions, $NH_3$ levels usually do not vary much while mixing ratios of $HNO_3$ frequently increase from a morning low to peak at midday, and then decrease throughout the afternoon. Less common at this site is to have north-northeast winds (Figure 1b) which resulted in a distinct $NH_3$ diel cycle starting with representative $NH_3$ mixing ratios in the morning, rapidly rising to a midday maximum, which decline throughout the afternoon and evening.

Previous studies have shown that the mixing of polluted and clean air masses commonly results in lognormal distributions of atmospheric species for one specific site, particularly for primary pollutants [e.g., *Georgopoulos and Seinfeld*, 1982; *Parrish et al.*, 1991]. Both the $HNO_3$ and $NH_3$ data sets contained a wide range of lognormally distributed values. Consequently, the mean values may be strongly influenced by a few very high values, in such cases, both mean and median values are plotted. Consolidation and hourly binning of this 1991-1995 summertime data set produced a composite mean diel cycle of $HNO_3$ at this site that is bimodal with nighttime and daytime mixing ratios of 400 and 900 pptv, respectively

(Figure 2a). The composite median $HNO_3$ diel cycle displays less variability (Figure 2a) on account of the low $HNO_3$ mixing ratios in NW surface winds (Figure 2b), which occurred twice as often as SW winds during our sampling (see Figure 2b and section 4.1). The same data processing procedure yielded composite average and median $NH_3$ diel cycles that show mixing ratios consistently in the 200-400 pptv range (Figure 2a).

### 3.2. Wind Sector and Season

Diel changes in the $HNO_3$ mixing ratio for the southwest (SW) and northwest (NW) wind sectors are of the order of 2000 and 500 pptv, respectively (Figure 2b). In addition to having a lower amplitude, the NW diel cycle also starts from lower baseline $HNO_3$ mixing ratios. This pattern matches that previously noted by *Munger et al.* [1996], for $NO_Y$ and $NO_X$, who defined the primary surface-wind direction sectors at this site as the north-northwesterly (270°-45°), the southwesterly (180°-270°), and the easterly (45°-180°). The $NH_3$ diel cycle did not change as a function of wind sector (not shown). However, mean and median mixing ratios of $NH_3$ and $HNO_3$ are different for the NW and SW wind sectors (Table 2). On average, an air mass with surface winds from the SW wind sector contains 3-4 times more $HNO_3$ and significantly less $NH_3$ ($p$ = 0.038) than one with winds from the NW wind sector (Table 2).

**Table 2.** Summary Statistics of Mixing Ratios at UNH Sampling Times and Selected Surface Wind Direction Sectors

| Statistic | All Samples | NW | E | SW |
|---|---|---|---|---|
| | | *$HNO_3$, pptv* | | |
| *n* | 766 | 367 | 146 | 177 |
| 25% | 211 | 154 | 279 | 453 |
| Median | 410 | 273 | 476 | 1239 |
| Mean | 817 | 484 | 650 | 1700 |
| s.d. | 1025 | 587 | 532 | 1533 |
| 75% | 984 | 539 | 854 | 2534 |
| | | *$NH_3$, pptv* | | |
| *n* | 463 | 234 | 90 | 113 |
| 25% | 142 | 179 | 133 | 124 |
| Median | 245 | 281 | 194 | 224 |
| Mean | 231 | 353 | 309 | 292 |
| s.d. | 254 | 260 | 229 | 266 |
| 75% | 452 | 471 | 467 | 436 |
| | | *$NO_X$, pptv* | | |
| *n* | 443 | 231 | 110 | 81 |
| 25% | 782 | 641 | 1406 | 1979 |
| Median | 1458 | 910 | 3396 | 4078 |
| Mean | 3647 | 1340 | 5214 | 8080 |
| s.d. | 7011 | 1221 | 6737 | 12844 |
| 75% | 3794 | 1522 | 6091 | 7497 |
| | | *$NO_Y$, pptv* | | |
| *n* | 662 | 359 | 135 | 156 |
| 25% | 1861 | 1485 | 3228 | 3616 |
| Median | 3481 | 2290 | 4484 | 5592 |
| Mean | 5191 | 3038 | 6871 | 8655 |
| s.d. | 5947 | 2428 | 5875 | 9022 |
| 75% | 6099 | 3772 | 8557 | 10972 |
| | | *{$NO_Y$-$NO_X$}, pptv* | | |
| *n* | 395 | 227 | 92 | 69 |
| 25% | 992 | 976 | 933 | 1015 |
| Median | 1793 | 1629 | 2095 | 2457 |
| Mean | 2466 | 1985 | 2952 | 3429 |
| s.d. | 2266 | 1468 | 2963 | 2942 |
| 75% | 3017 | 2548 | 3412 | 5483 |

Northwest (NW) is 270°-45°, East (E) is 45° - 180°, and Southwest (SW) is 180°-270°. Statistics include number of samples (*n*), 25th percentile (25%), standard deviation (s.d.), and 75th percentile (75%).

Since a backwards trajectory analysis was not performed for these sample periods, it is difficult to ascribe a specific source region to a particular gas sample. However, it is possible to observe that easterly winds form the general Boston metropolitan area were quite rare during our sampling and were commonly associated with low-pressure systems off the coast. A situation where "fresh" industrial emissions could have been rapidly transported to the site during overcast conditions consequently resulting in low $HNO_3$ (Figure 3) and high $NO_X$ mixing ratios [*Munger et al.*, 1996].

Over a 5 year period the majority (66%) of $HNO_3$ samples were collected in the summer (June, July, August) while 23% and 10% of the samples were collected in spring (March, April, May) and fall (September, October, November), respectively. No samples were collected in the winter (December, January, February). The measured $HNO_3$ mixing ratios were lowest in early spring (Figure 4a) and highest in late summer to early fall (days 210-240 of 1994). The $NH_3$ levels peak in July and August (Figure 4b) with lower mixing ratios observed in the spring. An exponential relationship ($r^2$ = 0.82) between $NH_3$ levels and air temperature is evident for the summer of 1995 (Figure 5). At times the temperature dependence of the $NH_3$ breaks down, as shown for August 1995 (Figure 5). Data from other earlier years contain similar dual temperature relationships, but for purposes of clarity, only one year of summertime $NH_3$ data is included in Figure 5.

## 4. Discussion

### 4.1. Representativeness of the Composite Data Set

To extract meaning from a noncontinuous data set it is necessary to determine what time period the composite data set most closely represents. Certainly, the mean and median values reported in Table 2 are not necessarily comparable to overall annual values due to the lack of wintertime (December - February) data (Table 1). Due to the availability of a continuous data set of many chemical species and meteorological parameters made by Harvard University (HU) from the same tower, [e.g., *Munger et al.*, 1996, 1998) we can investigate how a parameter measured more or less continuously between 1991 and 1995 compares to the same parameter analyzed only for the UNH composite sampling times.

Measurements of wind direction reveal that NW winds occur 49% and 52% of the time for continuous (HU) and composite (UNH) sampling, respectively. Similar good agreement is observed for the E and SW windsectors (Table 3). However, it appears that the SW sector is underrepresented (Δ -12%) and NW similarly over represented (Δ 8%) in the composite data set when compared to summer-only HU observations (Table 3). On a diel basis, the median $NO_Y$ measured during UNH sampling times compares well with the median summertime $NO_Y$ diel (Figure 6), with the greatest differences occurring in the nighttime hours when UNH sample coverage

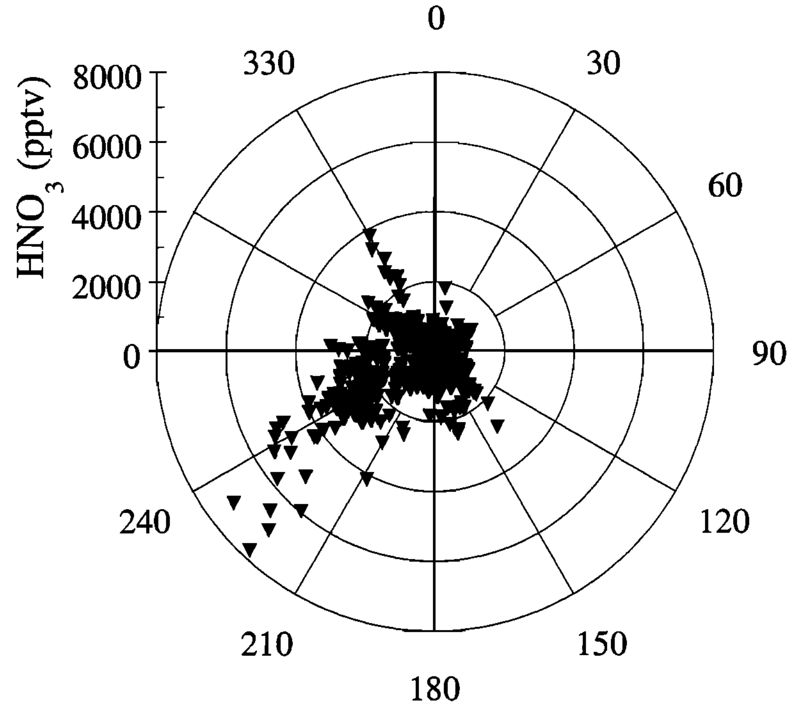

Figure 3. $HNO_3$ mixing ratios ($n$ = 711) as a function of average hourly wind direction (degrees). $HNO_3$ mixing ratio uncertainly of ± 11% not shown to improve readability.

was the lightest (Figure 2a). Summer and winter $NO_Y$ diel cycles vary considerably [*Munger et al.*, 1996]; consequently, the UNH composite $NO_Y$ diel cycle between 0900 and 1300 is significantly different ($p < 0.05$) from the 1991-1995 mean annual $NO_Y$ diel. Overall, the composite data set is most representative of summer conditions between the hours of 0500 and 2000 with a bias toward air masses with surface winds from the cleaner NW sector.

### 4.2. $HNO_3$

**4.2.1. Comparison to other measurements.** Table 4 is a compilation of $HNO_3$ measurements in rural North America, sorted in order of increasing sample integration time. This list, while not exhaustive, represents some of the more recent measurements. All the results, with the exception of this study, were obtained using Teflon/Nylasorb filterpacks which have previously been shown to compare reasonably well to the MC/IC technique [*Talbot et al.*, 1990]. When comparing these values, note that all the subdaily measurement campaigns mainly occurred during the summer months. Many of these high-resolution projects do not include nighttime measurements (as noted in Table 4) which are generally lower [*Edgerton et al.*, 1992] and may be biased by nonrepresentative meteorological conditions. While the daily and weekly $HNO_3$ sampling programs provide excellent seasonal and annual coverage, the long integration times may mask hourly and day/night variability that is useful in understanding the processes influencing the atmospheric chemistry of $HNO_3$.

The overall hourly mean and median $HNO_3$ mixing ratio for Harvard Forest agrees quite well with other measurements in rural North America (Table 4). The large range of $HNO_3$ mixing ratios (26-7771 pptv) at Harvard Forest is indicative of the wide variety of air masses that influence this site. The smaller $HNO_3$ variability reported in most other studies is to some degree a consequence of longer sample integration times, especially the weekly sampling of the National Dry Deposition Network [*Edgerton et al.*, 1992] which has now been incorporated into the EPA Clean Air Status and Trends Network (CASTNet). *Ollinger et al.* [1993] noted that mean $HNO_3$ levels for the CASTNet sites in the northeastern United States decreased linearly with increasing latitude. Interestingly, Harvard Forest at 42.5°N with a mean hourly mixing ratio of 828 pptv fits this trend (Table 4). The gradient of decreasing $HNO_3$ values to the north of this site concurs with the calculations of *Munger et al.* [1998], who concluded that much of the $NO_X$ emitted in the northeastern United States is deposited as $HNO_3$ within a few days.

**4.2.2. $HNO_3$ diel trends.** $HNO_3$ mixing ratios are lower at night and higher during the day at Harvard Forest (Figure 2a) and at other sites as well [*Edgerton et al.*, 1992; *Parrish et al.*, 1986]. Previous attempts to define the diel cycle of $HNO_3$ have shown similar patterns, with the highest mixing levels occurring in the afternoon [*Parrish et al.*, 1986; *Aneja et al.*, 1994a, *Kleinman et al.*, 1994]. The distinctly different $HNO_3$ diel patterns for the SW and NW windsectors emphasize the respective urban and rural source regions for these air mass categories (Figure 2b). Earlier studies at Harvard Forest [e.g. *Munger et al.*, 1996] labeled the SW and NW surface wind direction sectors as "polluted" and "clean" based on significantly higher midday $NO_X$ and $NO_Y$ mixing ratios for the SW sector. Using a trajectory model, *Moody et al.* [1998] quantitatively determined the same air masses source regions and described their divergent chemical climatologies. Instead of using a meteorological parameter, *Kleinman et al.* [1994]

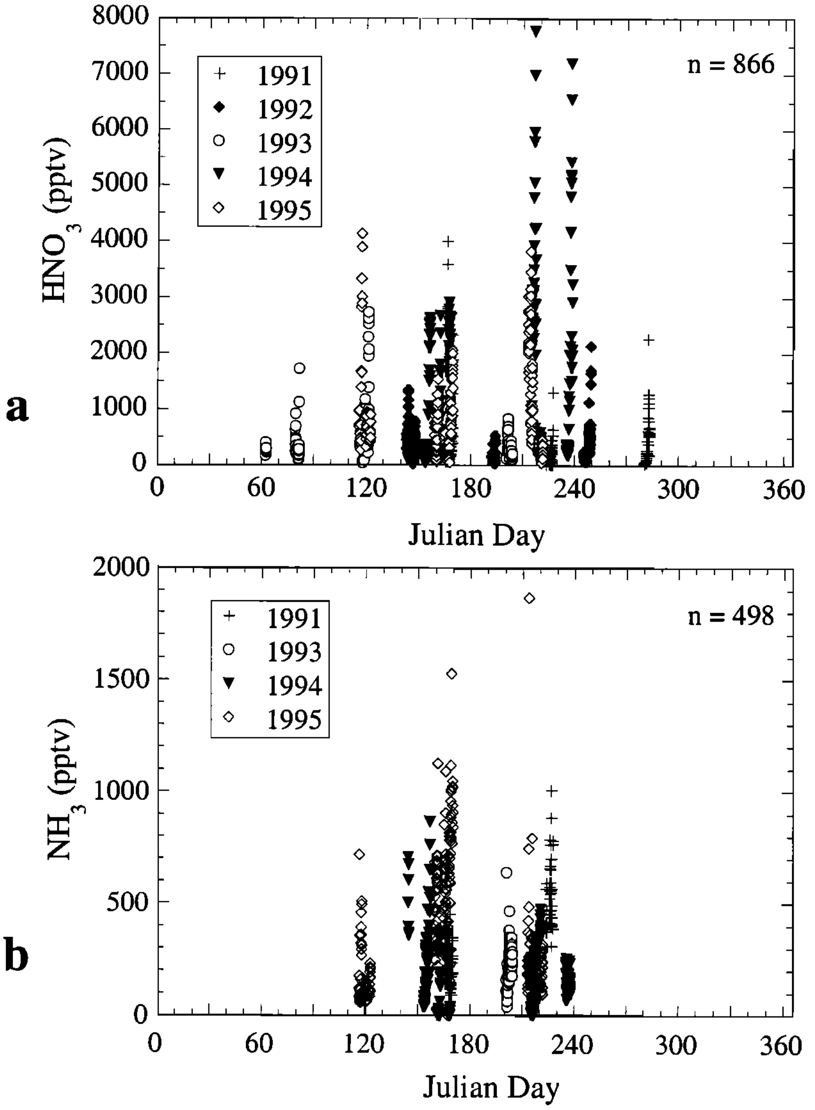

**Figure 4.** (a) Hourly integrated $HNO_3$ mixing ratios plotted versus Julian day. All samples collected between 1991 and 1995 on days listed in Table 1. Measurement uncertainty of ±11% not shown to keep figure legible. (b) Same as Figure 4a, except for $NH_3$. Measurement uncertainty of 17% not shown.

subdivided $HNO_3$ data from rural Georgia into groups based on $O_3$ mixing ratios and in the process produced two $HNO_3$ diel patterns of similar shape and magnitude to those in Figure 2b.

The notable rise in early morning $HNO_3$ mixing ratios (~ 0500 LT) (Figures 2a and 2b) is coincident with average time of summer sunrise as well as large increases in the heat flux, friction velocity, $NO_X$ and $NO_Y$ mixing ratios, and $NO_Y$ deposition rate [*Munger et al.*, 1996]. Due to low photochemical activity at this time of day, it is likely that this increase in $HNO_3$ could result from the entrainment of $HNO_3$ in "fossil" mixed layer air from the previous day as the new mixed layer develops [*Kleinman et al.*, 1994]. Large increases in early morning $NO_Y$ deposition velocities [*Munger et al.*, 1996] endorse this theory by demonstrating high concentrations of a readily depositing $NO_Y$ species (e.g., $HNO_3$) in these air masses. *Trainer et al.* [1991] predict that some of the $HNO_3$ mixed down as the nocturnal boundary layer erodes is produced at night via heterogeneous reactions involving $N_2O_5$.

**4.2.3. Seasonal differences in $HNO_3$.** *Munger et al.* [1998] analyzed 7 years (1990-1996) of continuous hourly $NO_Y$ flux measurements at this site and report the highest $NO_Y$ deposition occurs during the months of May, July, and August and the lowest during December, January, and February. As the primary depositing species of $NO_Y$, the composite $HNO_3$ seasonal cycle (Figure 4a), while lacking wintertime data, is consistent with these findings. *Parrish et al.* [1986] also report their maximum and minimum $HNO_3$ levels in late summer and winter, respectively. However, other studies from other regions have observed the significantly different $HNO_3$ seasonal cycles. In Cedar Creek, Wyoming, the highest levels occur in the spring [*Edgerton et al.*, 1992], while Bondville and Argonne, Illinois experience their peak $HNO_3$ concentrations in the winter [*Meyers et al.*, 1991]. Seasonal differences in $HNO_3$ are believed to be a function of many interrelated physical and climatological factors which may also differ seasonally and geographically, including: homogeneous and heterogeneous production, dry deposition and wet removal, local

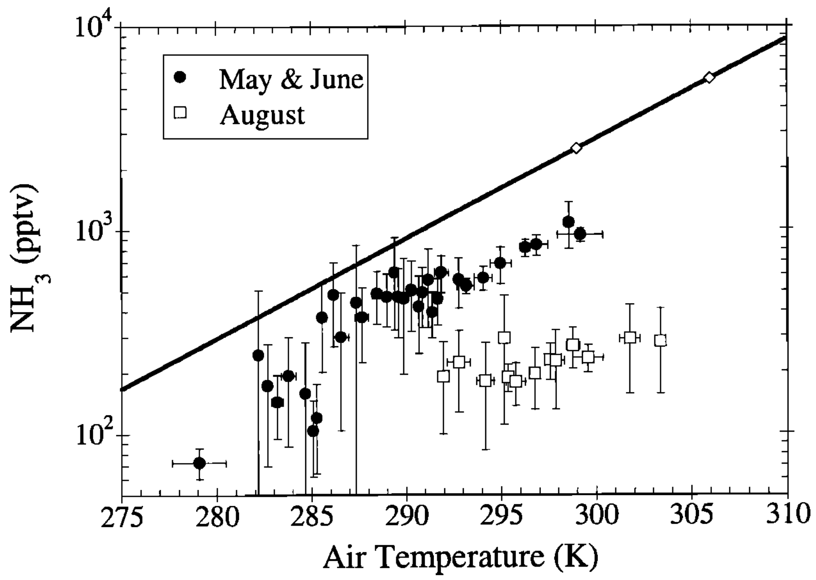

**Figure 5.** Temperature dependence of gaseous $NH_3$ mixing ratios collected for two different periods in the summer of 1995: May 1 to June 18, 1995 (May, June) and August 1-9, 1995 (August). Each symbol represents the average of five individual 1 hour measurements spanning the temperature range indicated by the horizontal bars. The vertical bars represent the standard deviation of the five samples. The solid line corresponds to the calculated $NH_3$ vapor pressure above a solution with 46 μM [$NH_4^+$] and *p*H 6.8 [*Farquhar et al.*, 1980].

biogenic isoprene emissions, boundary layer dynamics, and regional $NO_X$ emission densities.

While the weekly CASTNet samples will probably not be useful to determine the importance of some of these factors such as nighttime heterogeneous $HNO_3$ production, it is a good data set to examine seasonal $HNO_3$ levels across the eastern United States. The 1994 data from two northeastern United States CASTNet sites (Howland, Maine and Abington, New York) were selected to highlight the two extremes in the regional $HNO_3$ latitudinal gradient. In 1994, both of these sites report the highest sustained $HNO_3$ levels in July and August (~ days 180-240) (Figure 7) and lower mixing ratios in the winter, which is consistent with the $HNO_3$ and $NO_Y$ deposition results at Harvard Forest [this study; *Munger et al.*, 1998]. Peak July and August $HNO_3$ mixing ratios at Harvard Forest and other northeastern sites may be explained by additional $HNO_3$ production via organic nitrate pathways [*Munger et al.*, 1998]. The coherence of the $HNO_3$ signals from these two sites, for both the long- and short-term (episodic) events, suggests that similar factors control the $HNO_3$ levels throughout the northeastern United States. The regional $HNO_3$ concentration gradient reported by *Ollinger et al.* [1993] is also evident in these two records and most likely represents the deposition of $HNO_3$ as a large portion of the emitted $NO_X$ is oxidized to $HNO_3$ and deposited within the region [*Munger et al.*, 1998].

**Table 3.** Frequency of Average Hourly Surface Winds by Sector (1991-1995)

| | | Frequency, % | | |
|---|---|---|---|---|
| | *n* | NW | E | SW |
| UNH[a] | 720 | 52 | 20 | 27 |
| 1991-1995[b] | 33330 | 49 | 19 | 32 |
| Summer (1991-1995)[c] | 8466 | 44 | 16 | 39 |

Northwest (NW) is 270°-45°, East (E) is 45°-180°, and Southwest (SW) is 180°-270°.

[a] University of New Hampshire (UNH) $HNO_3$ and $NH_3$ sampling times.

[b] Harvard University continuous measurements.

[c] Summer is defined as June, July, and August.

### 4.3. $NH_3$

**4.3.1. Comparison to previous $NH_3$ measurements.** The mean $NH_3$ mixing ratio of 321 pptv is equivalent to the 300 and 420 pptv summertime mean observed for other forested sites in Oak Ridge, Tennessee and Niwot Ridge, Colorado [*Langford et al.*, 1992]. At Harvard Forest, 10 years previous to this study, *Tjepkema et al.* [1981] observed summertime $NH_3$ mixing ratios in the range of 200-330 pptv using 7 day oxalic acid denuder measurements. The greater variability displayed in our hourly measurements is due to the damping of high-frequency structure by the weekly integrated samples.

Our composite $NH_3$ diel cycle does not display the trend of higher daytime mixing ratios peaking in the afternoon and then gradually declining throughout the night observed at several other sites [*Langford et al.*, 1992]. Some of the individual days that went into this composite do, however, demonstrate such a pattern, including day 165 of 1995 as shown in Figure 1b. Interestingly, some days with a flat $NH_3$ diel cycle display a more "typical" $NH_X$ ($NH_3$ + $NH_4^+$) diel signal (Figure 8a).

Our composite of summer $NH_3$ levels generally fits in with the complete year of $NH_3$ concentrations measured *by Tjepkema et al.* [1981] at Harvard Forest in 1980. They found the highest $NH_3$ levels to occur in the summer, peaking in early August and decreasing rapidly to fall and winter lows of less than 50 pptv. As suggested by the "typical" seasonal and diel cycles of $NH_3$, boundary layer $NH_3$ levels are a general func-

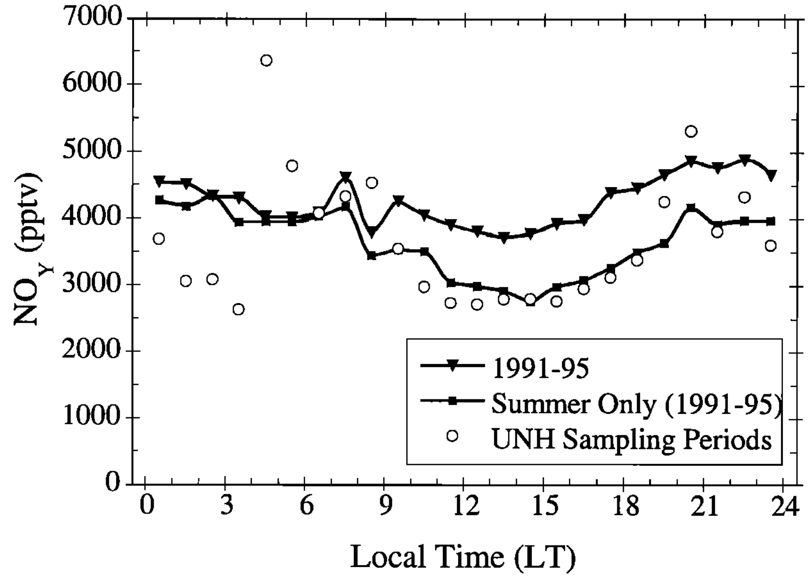

**Figure 6.** Median diel cycles of $NO_Y$ between 1991 and 1995 for three different sets of data: all data; summertime only (June, July, and August); and UNH $HNO_3$ sampling periods listed in Table 1. Number of samples in each hourly group is ≈ 1200 for 1991 and 1995 and ≈ 350 for summer only. UNH sample number shown in Figure 2a for $HNO_3$ sampling times.

tion of air temperature, with higher $NH_3$ mixing ratios associated with warmer temperatures [*Langford et al.*, 1992]. Our observations of small, or no, diel variation of $NH_3$ mixing ratios on many days suggests that other factors also play a significant role in regulating $NH_3$ levels at the Harvard Forest.

**4.3.2. Controls on boundary layer $NH_3$ levels.** It is clear that air temperature is a primary controller of $NH_3$ in the boundary layer, as several other sites show a strong temperature dependence on $NH_3$ mixing ratios [*Langford et al.*, 1992]. Higher air temperatures lead to greater emissions of $NH_3$ from its primary sources, cattle feedlots and fertilizer applications. As ambient $NH_3$ mixing ratios above vegetated systems approach the $NH_3$ compensation point, higher air temperatures increase the vapor pressure of $NH_3$ above the $NH_4^+$ dissolved in the water film lining stomatal cavities, increasing the $NH_3$ emitted by the canopy as predicted by Henry's Law [*Langford and Fehsenfeld*, 1992]. At Harvard Forest, due to the lack of nearby sources and high levels of $SO_4^{2-}$ in the atmosphere, the ambient mixing ratios of $NH_3$ are more or less always below the $NH_3$ compensation point reported by *Farquhar et al.* [1980], suggesting that the canopy (or ecosystem) at Harvard Forest may be continually losing $NH_3$ to the atmosphere. Similarly, based on the low nature of the few $NH_3$ mixing ratios reported for eastern forests, *Lang-*

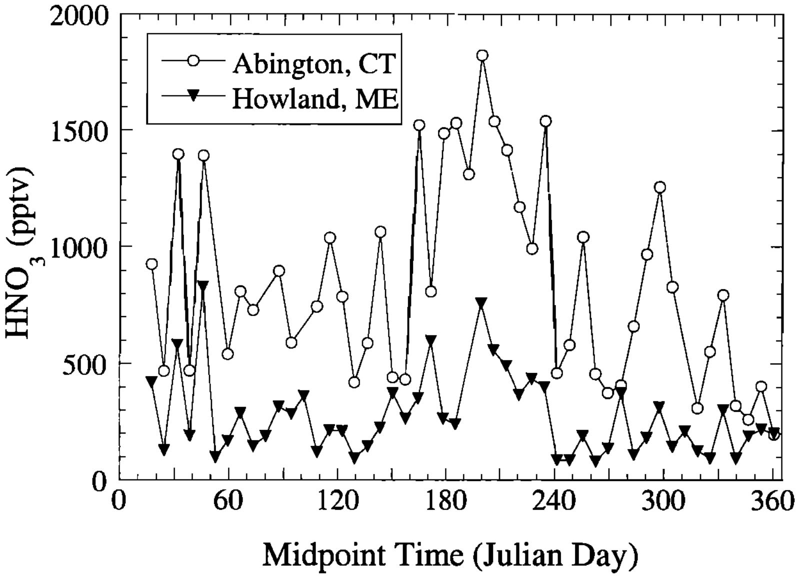

**Figure 7.** Weekly integrated $HNO_3$ mixing ratios for 1994 for two northeastern sites. Data are from U.S. EPA Clean Air Status and Trends Network (CASTNet) sites in Abington, Connecticut (ABT147) and Howland, Maine (HOW132) [*Clean Air Status and Trends Network*, 1997].

**Table 4.** Nitric Acid Mixing Ratios for Various Sites in Rural North America

| Site (Latitude) | Mean ± s.d. (Median ± MAD) | Range | Integration (Restrictions) Study Period | Method | Source |
|---|---|---|---|---|---|
| Harvard Forest, Massachusetts (42.5°N) | 828±1045, (423±257) | 26-7771 | 1 hour (episodic), Summers 1991-1995 | Mist Chamber | This Study |
| Candor, North Carolina (35.3°N) | 670±330 | 30-1760 | 1 hour (daytime only), June-July 1992 | Teflon/nylon filter pack | *Aneja et al.* [1994b] |
| Metter, Georgia (32.4°N) | 800 | | 1 hour, June - August 1991 | $NO_Y$-$NO_Y$ with nylon Filter (includes particulate $NO_3^-$) | *Kleinman et al.* [1994] |
| Mt. Mitchell, North Carolina (35.8°N) | 406±340 (1988)<br>498±210 (1989) | 20-2000 | 2 hours (daytime only), summers 1988-1989 | Teflon/nylon filter pack | *Aneja et al.* [1994a] |
| Niwot Ridge, Colorado (40.3°N) | ---- | 10-3000 | 1-4 hours (daytime only), all seasons 1979-84 | Teflon/nylon filter pack | *Parrish et al.* [1986] |
| Oak Ridge, Tennessee (36.0°N) | 1649 | 697-2819 | 4 hour (daytime only), September 1982 | Teflon/nylon filter pack | *Meyers et al.* [1989] |
| Calgary, Alberta (51.0°N) | 420 | 20-4000 | 4 hours (daytime only), June-August 1982 | Teflon/nylon filter pack | *Peake et al.* [1985] |
| Pittsburg, California (38.0°N) | ---- | 300-1500 | 8 hours, February 1979 | Teflon/nylon & Teflon/NaCl filter pack | *Appel et al.* [1980] |
| Whiteface Mountain, New York (44.3°N) | 200 (clean)<br>1000 (polluted) | 100-3100 | 6/12 hours, July 1982 | Teflon/NaCl filter pack & diffusion denuder | *Kelly et al.* [1984] |
| State College, Pennsylvania (40.8°N) | 900 (January)<br>400 (February)<br>500 (March) | 50-1400 (January)<br>100-810 (February)<br>100-2295 (March) | 24 hours (15 days/month), January-March 1984 | Teflon/nylon filter pack downstream of $NH_3$ denuder | *Lewin et al.* [1986] |
| Niwot Ridge, Colorado (40.3°N) | 64 (Winter)<br>238 (Summer) | 20-700 | 24 hours (episodic), All Seasons 1980-1984 | Teflon/nylon filter pack | *Parrish et al.* [1986] |
| Howland, Maine (45.2°N) | 270±174$^a$<br>425±154$^b$ | 79-829$^a$<br>154-329$^b$ | 7 days, January 1993-present | Teflon/nylon filter pack | *CASTNet* |
| Woodstock, New Hampshire (43.5°N) | 241±123$^a$<br>256±80$^b$ | 58-605$^a$<br>162-398$^b$ | 7 days, January 1989-present | Teflon/nylon filter pack | *CASTNet* |
| Lye Brook, Vermont (43.0°N) | 677±331$^a$<br>733±218$^b$ | 201-1409$^a$<br>352-1124$^b$ | 7 days, April 1994-present | Teflon/nylon filter pack | *CASTNet* |
| Connecticut Hill, New York (42.4°N) | 921±324$^a$<br>1038±359$^b$ | 297-1911$^a$<br>612-1911$^b$ | 7 days, October 1987-present | Teflon/nylon filter pack | *CASTNet* |
| Catskills, New York (42.4°N) | 975±412$^a$<br>1165±232$^b$ | 291-1665$^a$<br>736-1615$^b$ | 7 days, May 1994-present | Teflon/nylon filter pack | *CASTNet* |
| Abington, Connecticut (41.9°N) | 842±430$^a$<br>1232±440$^b$ | 197-1822$^a$<br>430-1822$^b$ | 7 days, December 1994-present | Teflon/nylon filter pack | *CASTNet* |

All mixing ratios reported as pptv.

CASTNet is the Clean Air Status and Trends Network [1997]. Only selected New England sites of CASTNet are presented.

[a] Annual for 1994.

[b] Summer for 1994.

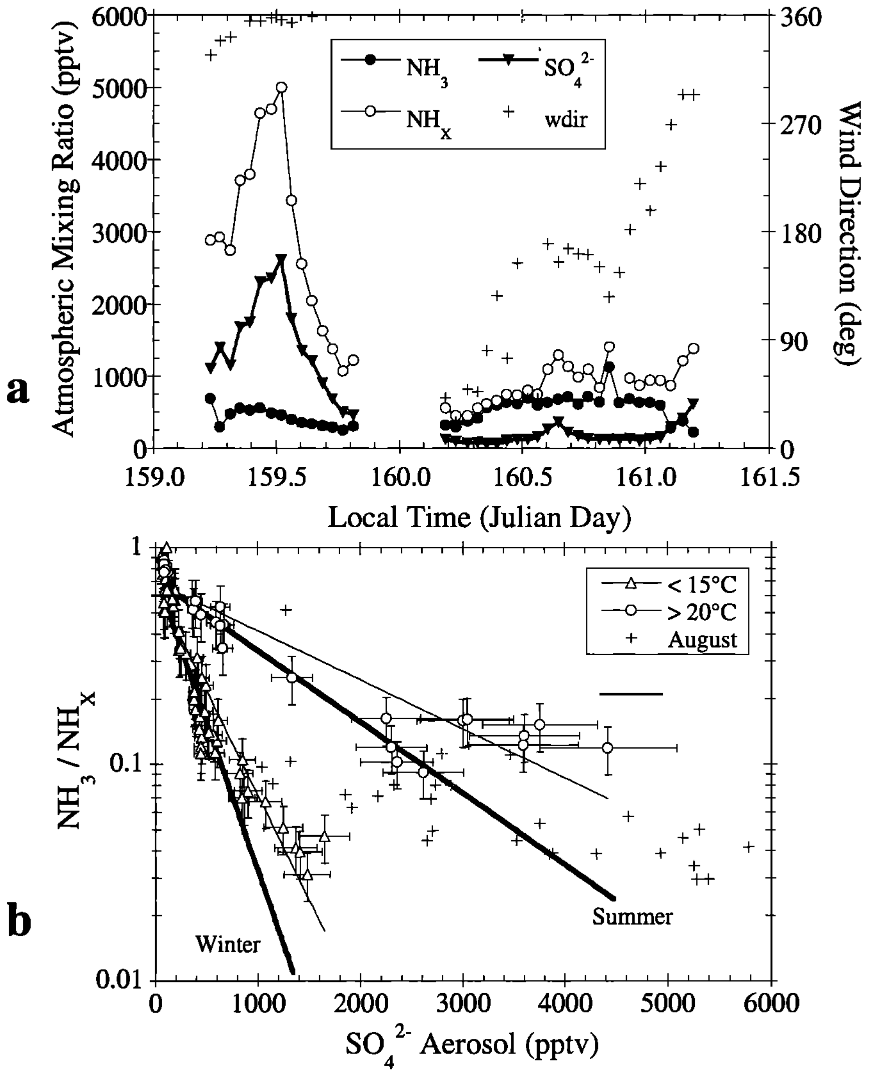

**Figure 8.** (a) Dependence of gaseous/particulate partitioning of ammonia on atmospheric sulfate. Wind direction and hourly $NH_3$ and $NH_X$ and aerosol $SO_4^{2-}$ mixing ratios for June 8 and 9, 1995 (J.D. 159 and 160). Measurement uncertainty not shown. (b) Dependence of $NH_3/NH_X$ partitioning on atmospheric sulfate and air temperature. Open symbols represent samples collected in May and June 1995 at two different temperature ranges (≤15°C (triangles) and ≥20°C (circles)). Vertical bars show the uncertainty of the partition ratio as determined by propagation of errors. Horizontal bars represent $SO_4^{2-}$ measurement uncertainty. Pluses correspond to August 1995 samples. Error bars for these samples are not shown to keep figure legible. Thick lines represent relationships reported by *Langford et al.* [1992] from a compilation of winter and summer results.

*ford et al.* [1992] predicted these ecosystems could emit significant levels of $NH_3$.

For the months of May and June of 1995, the exponential relationship between averaged $NH_3$ mixing ratios and temperature ($r^2$=0.85) may perhaps define the $NH_3$ compensation point for this ecosystem. If so, this particular $NH_3$ compensation point is lower than that previously observed *by Farquhar et al.* [1980] for snap beans and confirmed *by Langford and Fehsenfeld* [1992] for a lodgepole-ponderosa pine/ spruce-fir forest. The *Farquhar et al.* [1980] $NH_3$ compensation point is plotted as a function of air temperature for comparison (Figure 5).

Another fundamental determinant of $NH_3$ levels at most sites is their proximity to $NH_3$ sources. With mean and median mixing ratios between 200 and 350 for all wind sectors, this suggests that there are few significant sources of $NH_3$ near Harvard Forest. While mean $NH_3$ levels from the "clean" NW sector are significantly greater than those from the "polluted" SW sector, total $NH_X$ levels, and therefore total $NH_3$ emissions, are greater in the SW wind sector. Thus significant levels of $NH_3$ are emitted from the SW sector; however, a large fraction of the $NH_3$ is soon converted to $NH_4^+{}_{[p]}$, resulting in low ambient $NH_3$ mixing ratios.

As described earlier in section 2.3, $NH_3$ can rapidly react with $H_2SO_4$ to produce ammonium (bi)sulfate aerosols. In an acidic atmospheric environment dominated by $SO_4^{2-}$, *Tang* [1980] predicted that a primary control on the gaseous/particulate partitioning of ammonia is the level of atmospheric $SO_4^{2-}$. This control is clearly demonstrated by comparing two consecutive days (J.D. 159-160) in 1995. On day

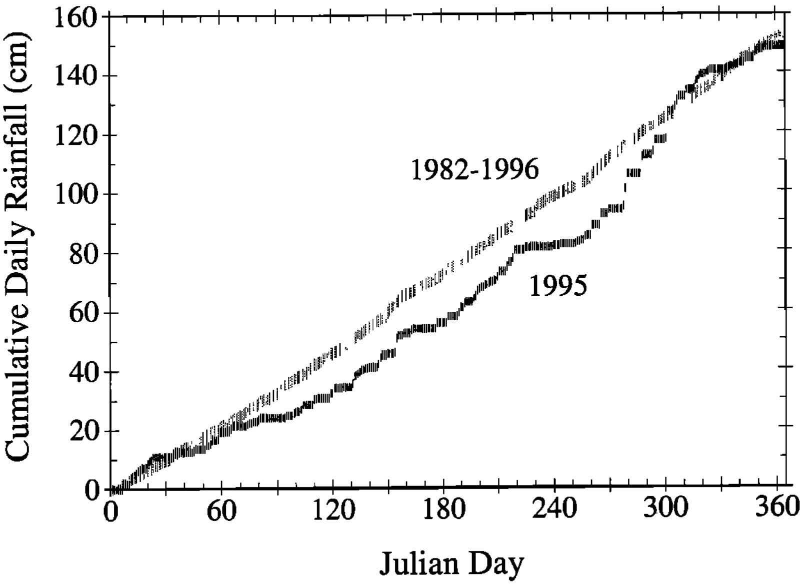

Figure 9. Cumulative daily rainfall at the Quabbin Reservoir National Atmospheric Deposition Program site for 1995 and 14 year average for years 1982-1996 [*National Atmospheric Deposition Program*, 1997].

159 (1995), north winds brought high levels of NH$_X$ (3-5 ppbv) and high SO$_4^{2-}$ levels (~ 1-2 ppbv) to Harvard Forest (Figure 8a) and NH$_3$ accounts for 9-25% of NH$_X$. On day 160, easterly winds advected moderate levels of NH$_X$ (~ 500-800 pptv) and very little aerosol SO$_4^{2-}$ (<500 pptv) resulting in the opposite situation with the majority of the NH$_X$ (67-91%) present as NH$_3$ instead of aeroscl NH$_4^+$ (Figure 8a).

Average aerosol SO$_4^{2-}$ mixing ratios for the "polluted" SW sector are 2.3 times higher than the NW sector, resulting in significantly different ($p < 0.001$) mean (± standard deviation) NH$_3$/NH$_X$ ratios of 0.39 (±0.22) and 0.23 (±0.22) for the NW and SW wind sectors, respectively. *Langford et al.* [1992] collected available data from various studies which simultaneously determined NH$_3$, NH$_4^+$, and SO$_4^{2-}$ mixing ratios. Breaking up the data into wintertime and summertime measurements, they observed negative exponential relationships between the fraction of NH$_X$ as NH$_3$ and total atmospheric sulfate. The steeper slope of the wintertime data was attributed to decreased wintertime NH$_3$ emissions and the lower equilibrium vapor pressure of NH$_3$ over ammonium sulfate aerosols at colder temperatures.

Separating our May and June 1995 NH$_3$ data into two groups based on the air temperature, ≤15°C and ≥20 °C, we observed exponential relationships describing the partitioning of NH$_3$ and NH$_4^+$ as a function of SO$_4^{2-}$$_{[p]}$ (Figure 8b). The squared correlation coefficients are 0.85 and 0.90 for the ≤15°C and ≥20°C groups, respectively. These relationships are quite similar to those reported by *Langford et al.* [1992], which, for comparison, have been included in Figure 8b (thicker lines). Not included in this analysis, but also shown in Figure 8b, are NH$_3$ data from August 1995. All the data collected during August represent sampling periods in which the air temperature was 19°C or greater. With the exception of the samples with quite high SO$_4^{2-}$ mixing ratios (> 3500 pptv), most of the remaining August samples fall somewhere between the ≤15°C and ≥20 °C ammonia-to-sulfate relationships described above. August 1995 is the same period for which the relationship between NH$_3$ and temperature shown in Figure 5 does not apply.

In addition to being a warmer time period (Figure 5), the August samples also contained on average significantly more SO$_4^{2-}$ and less NH$_3$ relative to NH$_4^+$ (Figure 8b). However, the majority of the August samples were collected within temperature and SO$_4^{2-}$ ranges observed during summer and still contained less NH$_3$ (Figures 5 and 8b). *Langford and Fehsenfeld* [1992] also observed a deviation from the predicted compensation point at higher temperatures and speculated that lower NH$_3$ emissions were related to water stress. At Harvard Forest, 1995 was drier than average with a period of drought occurring from early August through mid-September as shown by cumulative daily rainfall (Figure 9). These data further suggest that for vegetation experiencing water (or other physiological) stress, which encourages reduced stomate aperatures, the exchange of NH$_3$ is also restricted, effectively suppressing a plant's NH$_3$ compensation point.

Alternatively, recent studies have investigated the equilibrium vapor pressure of NH$_3$, HNO$_3$, or H$_2$SO$_4$ over ammonium nitrate and ammonium sulfate solutions [e.g., *Clegg et al.*, 1998]. For our data set, the product ($K$) of [HNO$_3$] and [NH$_3$] is considerably lower than the calculated ammonium nitate dissociation constant ($K_C$) of *Stelson and Seinfeld* [1982] at all relative humidities and temperatures. Studies by *Marti et al.* [1997] have shown that the vapor pressure of H$_2$SO$_4$ decreases dramatically when NH$_3$ is added to the sulfuric acid solution, suggesting that the vapor pressure of NH$_3$ over ammonium (bi)sulfate could also be low. A proper analysis of this complex multiphase system is beyond the scope of this paper and will hopefully be thoroughly investigated in a future study.

### 4.4. NO$_Y$ and HNO$_3$

The NO$_Y$ diel cycle at Harvard Forest, with lower mixing ratios at midday and higher levels at night, has been attributed

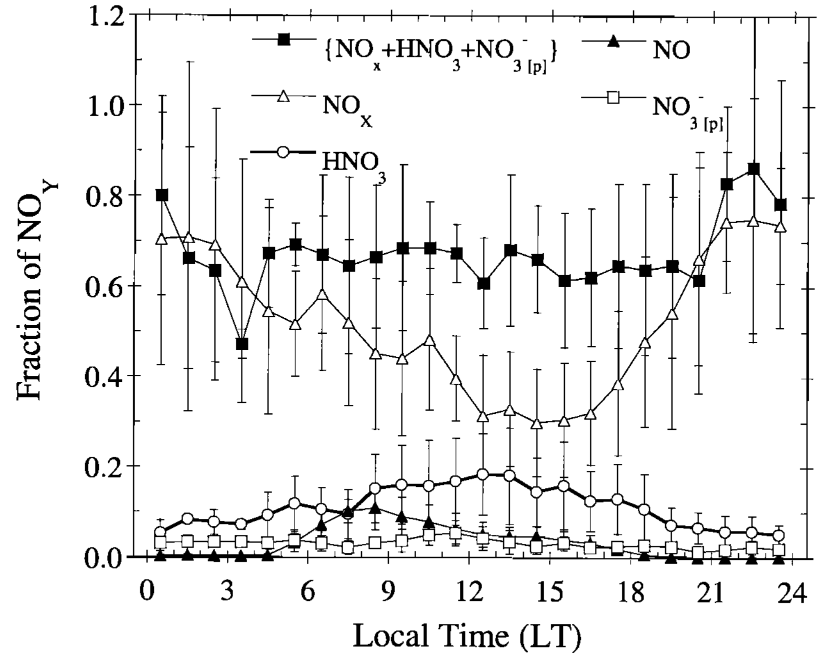

**Figure 10.** Median partitioning ratio of individual and sum of measured $NO_Y$ species as a function of time of day. Vertical bars represent median absolute deviation (MAD). Sample numbers for this composite diel are the same as $HNO_3$ diel in Figure 2a.

to changes in the height of the boundary layer and the vertical distribution of $NO_Y$ [*Munger et al.*, 1996]. At night, local anthropogenic $NO_X$ emissions accumulate below the stable nocturnal boundary layer. As the mixed layer grows the next morning, boundary layer $NO_Y$ concentrations are diluted by the entrainment of air lower in $NO_Y$ from aloft. For the UNH sampling periods this process resulted in median midday and midnight $NO_Y$ mixing ratios of ~ 3000 and 4000 pptv, respectively (Figure 6). The range of $NO_Y$ values and diel trend are similar to those observed at other flatland rural sites in North America [*Parrish et al.*, 1993].

Four of the individual component species of $NO_Y$ (NO, $NO_2$, $HNO_3$, and $NO_3^-{}_{(p)}$) were simultaneously measured at Harvard Forest. NO and $NO_2$ rapidly interconvert between each other as function of actinic flux, oxidant concentrations ($O_3$ and peroxy radicals), and temperature [*Parrish et al.*, 1993]. Thus when considering a composite data set collected under a variety of conditions, it is more meaningful to look at $NO_X$, the sum of NO and $NO_2$. $NO_X$ is, at all times, the largest fraction of $NO_Y$ at Harvard Forest (Figure 10).

At night $NO_X$ accounts for more than 60% of $NO_Y$ while no other measured species contributes more than a 10% share of $NO_Y$ (Figure 10). Nitric acid is the next most abundant measured $NO_Y$ species with a midday maxima of 20% of $NO_Y$ occurring at the same time as the $NO_X$ minima, indicative of the photochemical oxidation of $NO_2$ to $HNO_3$. At night, all the NO in the surface layer is titrated to $NO_2$ by reaction with $O_3$ and other oxidants. As the Sun rises, $NO_2$ photolysis begins and the NO contribution increases from essentially zero to a high of about 10% of $NO_Y$ around 0800 LT (Figure 10). Aerosol $NO_3^-$ is a minor fraction of $NO_Y$ at this site accounting for 3-7% of $NO_Y$ at any time of the day.

The sum of these four $NO_Y$ species ($\Sigma NO_{Y(i)}$) accounted for 60-80% of $NO_Y$, with the median of the unmeasured residual remaining fairly constant (~ 1500-2500 pptv) throughout the day (Figure 10). In air masses with winds from the urban SW wind sector, the mean (± standard deviation) "unmeasured" $NO_Y$ fraction ($NO_Y$ - $\Sigma NO_{Y(i)}$) was 23% (±14%) of $NO_Y$. The "unmeasured" $NO_Y$ fraction accounted for approximately 40% ± 20% of the $NO_Y$ in surface winds from the rural areas to the NW and from the Boston metropolitan area to the east. Typically, $NO_X$, $HNO_3$, and PAN are the major reactive nitrogen species at most sites [*Parrish et al.*, 1993]. Recent studies suggest that various other organic nitrates may also be an important component of $NO_Y$ at forested sites [*Trainer et al.*, 1991]. The majority of the "unmeasured" $NO_Y$ at Harvard Forest is most likely PAN and other organic nitrates. In contrast to $HNO_3$, PAN is only a temporary $NO_Y$ reservoir since it thermally decomposes back to $NO_X$. For a site in Scotia, Pennsylvania, situated in an oak forest, midday summertime PAN mixing ratios can get as high as 2000 pptv and can account for as much as 30-40% of $NO_Y$ [*Trainer et al.*, 1991]. Oak forests like Harvard Forest emit large amounts of isoprene in the summer months [*Goldstein et al.*, 1998]. Since the oxidation products of isoprene are thought to be important precursors of PAN [*Trainer et al.*, 1991], one would expect significant PAN levels at Harvard Forest. Since it quickly degrades at summertime surface temperatures, PAN tends to have a diel cycle similar to $HNO_3$. The diel cycle of the $NO_Y$ residual does appear to decrease in the evening (2200-0100) as expected (Figure 10). However, the larger variability in the nighttime values due to the lower sampling coverage make this a non-significant difference.

The quantity $\{NO_Y\text{-}NO_X\}$ describes the sum of $HNO_3$, PAN, and other oxidized reactive N species. The linear relationship between $HNO_3$ and $\{NO_Y\text{-}NO_X\}$ (slope = 0.55, $r^2$ = 0.86) indicates that $HNO_3$ is typically about half of the oxidized $NO_Y$ in air masses arriving from the SW wind sector

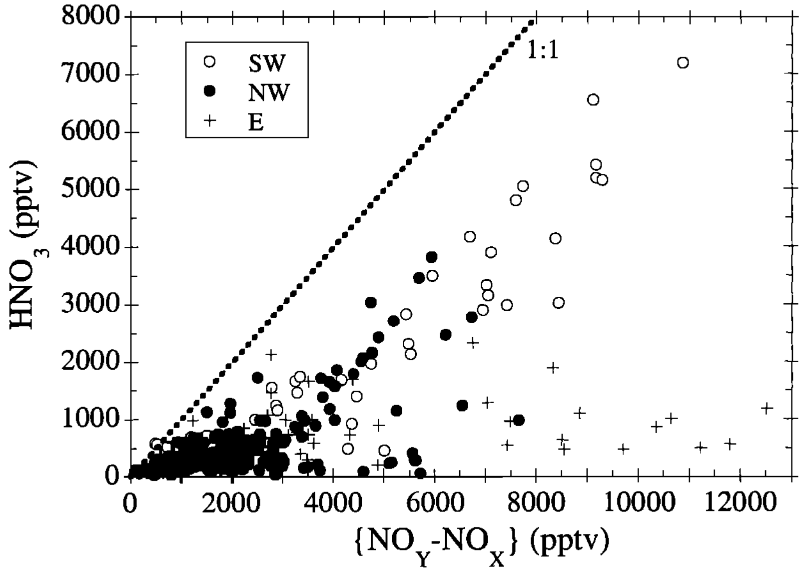

Figure 11. Relationship between $HNO_3$ and oxidized fraction of $NO_Y$, defined as $\{NO_Y\text{-}NO_X\}$, for the three surface wind sectors: 180°-270° is southwest (SW); 270°-45° is northwest (NW); 45°-180° is east (E). Error bars not shown.

(Figure 11). While more variable, on average about 25% of $\{NO_Y\text{-}NO_X\}$ is $HNO_3$ in the NW and E surface wind sectors. *Trainer et al.* [1991] modeled the photochemical production of organic nitrates, such as butyl and isoprene nitrates, and predicted that these reactive N compounds may contribute as much as 1000 pptv to $NO_Y$ at night and 3000 pptv or more to $NO_Y$ midday. These high levels appear possible in light of the unusual results observed for several early evening hours between April 27 and 30, 1993. During these hours an air mass with easterly surface winds contained less than 1 ppbv of $HNO_3$, 4-5 ppbv of $NO_X$, and more than 8 ppbv of "unidentified" oxidized $NO_Y$, presumably PAN and other organic nitrates (Figure 11).

## 5. Conclusions

Mean summertime $HNO_3$ mixing ratios at Harvard Forest agree well with results from other rural sites and fit in with the latitudinal $HNO_3$ gradient for the northeastern United States. This site receives air masses from both urban and rural source regions resulting in mean and median $HNO_3$ levels 4 times higher when surface winds were from the SW as opposed to the NW wind sector. High early morning $HNO_3$ and aerosol $NO_3^-$ mixing ratios suggest of the entrainment of these species from aloft into the newly developing mixed layer. A behavior consistent with theories of nocturnal heterogeneous $HNO_3$ production in the "fossil" mixed layer.

The importance of acidic $SO_4^{2-}$ aerosols in regulating the gaseous $NH_3$ levels at Harvard Forest is demonstrated by the low $NH_3$ mixing ratios and the exponential relationships between the $NH_3/NH_X$ partitioning ratio and aerosol $SO_4^{2-}$ concentrations. In the sulfate rich atmosphere above Harvard Forest, $NH_3$ mixing ratios appear to be suppressed below the $NH_3$ compensation point, suggesting that this N limited ecosystem may be losing N to the atmosphere through canopy $NH_3$ emissions. Air temperature is another factor controlling the $NH_3$ levels at this site. However, it is difficult to apportion the controls on $NH_3$ between the temperature response of the $NH_3$ compensation point and the temperature sensitivity of $NH_3/H_2SO_4$ production. The temperature response of these two controls may have similar results with warmer temperatures perhaps resulting in both greater $NH_3$ canopy emissions and a larger $NH_3/NH_X$ ratios for a given $SO_4^{2-}$ concentration.

On average $HNO_3$ makes up about 20% of $NO_Y$ at midday. PAN and perhaps other organic nitrates are believed to make up a significant fraction of $NO_Y$ at Harvard Forest since the sum of the measured $NO_Y$ species (NO, $NO_2$, $HNO_3$, and aerosol $NO_3^-$) typically account for between 60-80% of the summertime $NO_Y$ over the course of a day. $HNO_3$ makes up about half of the oxidized $NO_Y$ in polluted SW winds. However, unmeasured oxidized $NO_Y$ species comprise ~ 75% of the $\{NO_Y\text{-}NO_X\}$ in surface winds from the NW and E sectors, suggesting significant production of organic nitrates in these air masses.

**Acknowledgments.** This research was funded by the United States Department of Energy's (DOE) National Institute for Global Environmental Change (NIGEC) through the NIGEC Northeast Regional Center at Harvard University (DOE Cooperative Agreement DE-FC03-90ER61010). Financial support does not constitute an endorsement by the DOE of the views expressed in this article/report. The work at the University of New Hampshire (UNH) is supported by subcontract 901214-HAR#4 from Harvard University, under the Northeast Regional Center of NIGEC, to the Research Foundation of UNH. The excellent technical assistance of Eric Scheuer and thorough reviews of Jack Dibb are gratefully acknowledged. The insightful comments of two anonymous reviewers are also appreciated. The UNH gas and aerosol data set for Harvard Forest is available via anonymous ftp at io.harvard.edu and the Web site www-as.harvard.edu. This paper draws upon B. Lefer's dissertation submitted in partial fulfillment of the Doctor of Philosophy degree at the University of New Hampshire.

## References

Aneja, V.P., C.S. Clairborn, Z. Li, and A. Murthy, Trends, seasonal variations, and analysis of high-elevation surface nitric acid, ozone, and hydrogen peroxide, *Atmos. Environ.*, *28*, 1781-1790, 1994a.

Aneja, V.P., M. Das, D.-S. Kim, and B.E. Hartsell, Measurements and analysis of photochemical oxidants and trace gases in the rural troposphere of the southeast United States, *Is. J. Chem*, *34*, 387-401, 1994b.

Appel, B.R., and Y. Tokiwa, Atmospheric particulate nitrate sampling errors due to reactions with particulate and gaseous strong acids, *Atmos. Environ.*, *15*, 1087-1089, 1981.

Appel, B.R., S.M. Wall, Y. Tokiwa, and M. Haik, Simultaneous nitric acid, particulate nitrate and acidity measurements in ambient air, *Atmos. Environ.*, *14*, 549-554, 1980.

Appel, B.R., Y. Tokiwa, and M. Haik, Sampling of nitrates in ambient air, *Atmos. Environ.*, *15*, 283-289, 1981.

Appel, B.R., Y. Tokiwa, E.L. Kothny, R. Wu, and V. Povard, Evaluation of procedures for measuring atmospheric nitric acid and ammonia, *Atmos. Environ.*, *22*, 1565-1573, 1988.

Buhr, S.M., M.P. Buhr, F.C. Fehsenfeld, J.S. Holloway, U. Karst, R.B. Norton, D.D. Parrish, and R.E. Sievers, Development of a semi-continuous method for the measurement of nitric acid vapor and particulate nitrate and sulfate, *Atmos. Environ.*, *29*, 2609-2624, 1995.

Cadle, S.H., R.J. Countess, and N.A. Kelly, Nitric acid and ammonia in urban and rural locations, *Atmos. Environ.*, *16*, 2501-2506, 1982.

Clean Air Status and Trends Network (CASTNet) Database, Off. of Air and Radiat., U.S. Environ. Prot. Agency, Research Triangle Park, N.C., 1997.

Clegg, S.L., P. Brimblecombe, and A.S. Wexler, Thermodynamic model of the system $H^+$-$NH_4^+$-$SO_4^{2-}$-$NO_3^-$-$H_2O$ at tropospheric temperatures, *J. Phys. Chem.*, *102*, 2137-2154, 1998.

Cofer, W.R. III, V.G. Collins, and R.T. Talbot, Improved aqueous scrubber for collection of soluble atmospheric trace gases, *Environ. Sci. Technol.*, *19*, 557-560, 1985.

Crosley, D.R., Issues in the measurement of reactive nitrogen compounds in the atmosphere, *Rep. MP-94-035*, SRI Int., Menlo Park, Calif., March 1994.

Davies, C.N., The entry of aerosols into sampling tubes and heads, *Br. J. Appl. Phys.*, *1*, 921-932, 1968.

Davies, C.N., and M. Subari, Aspiration above wind velocity of aerosols with thin-walled nozzles facing at right angles to the wind direction, *J. Aeros. Sci.*, *13*, 59-71, 1982.

Denmead, O.T., J.R. Freney, and J.R. Simpson, A closed ammonia cycle within a plant canopy, *Soil Biol. Biochem.*, *8*, 161-164, 1976.

Dentener, F.J., and P.J. Crutzen, Reaction of $N_2O_5$ on tropospheric aerosols: Impact on the global distributions of $NO_X$, $O_3$ and OH, *J. Geophys. Res.*, *98*, 7149-7163, 1993.

Edgerton, E.S., T.F. Lavery, and R.P. Boksleitner, Preliminary data from the USEPA dry deposition network: 1989, *Environ. Pollut.*, *75*, 145-156, 1992.

Farquhar, G.D., P.M. Firth, R. Weselaar, and B. Weir, On the gaseous exchange of ammonia between leaves and the environment: Determination of the ammonia compensation point, *Plant Physiol.*, *66*, 710-714, 1980.

Forrest, J., D.J. Spandau, R.L. Tanner, and L. Newman, Determination of atmospheric nitrate and nitric acid employing a diffusion denuder with a filter pack, *Atmos. Environ.*, *16*, 1473-1485, 1982.

Georgopoulos, G.P., and J.H. Seinfeld, Statistical distribution of air pollutant concentrations, *Environ.l Sci. Technol.*, *15*, 401A-416A, 1982.

Goldstein, A.H., C.M. Spivakovsky, and S.C. Wofsy, Seasonal variations of nonmethane hydrocarbons in rural New England: Constraints on OH concentrations in northern latitudes, *J. Geophys. Res.*, *100*, 21,023-21,033, 1995.

Goldstein, A.H., M.L. Goulden, H.W. Munger, S.C. Wofsy, and C.D. Geron, Season course of isoprene emissions from a midlatitude deciduous forest, *J. Geophys. Res.*, in press, 1998.

Goulden, M.L., J.W. Munger, S.-M. Fan, B.C. Daube, and S.C. Wofsy, Exchange of carbon dioxide by a deciduous forest: Response to interannual climate variability, *Science*, *271*, 1576-1578, 1996.

Gschwandtner, G., K. Gschwandtner, K. Eldridge, C. Mann, and D. Mobley, Historic emissions of sulfur and nitrogen oxides in the United States from 1900 to 1980, *J. Air Pollut. Control Assoc.*, *36*, 139-149, 1986.

Hidy, G.M., Spatial and temporal distribution of airborne sulfate in parts of the U.S., *Atmos. Environ.*, *12*, 735-752, 1978.

Keene, W.C. et al., An intercomparison of measurement systems for vapor and particulate phase concentrations of formic and acetic acids, *J. Geophys. Res.*, *94*, 6457-6472, 1989.

Kelly, T.J., R.L. Tanner, L. Newman, P.J. Galvin, and J.A. Kadlecek, Trace gas and aerosol measurements at a remote site in the northeast U.S., *Atmos. Environ.*, *18*, 2565-2576, 1984.

Kleinman, L., et al., Ozone formation at a rural site in the southeastern United States, *J. Geophys. Res.*, *99*, 3469-3482, 1994.

Klemm, O., and R.W. Talbot, A sensitive method for measuring atmospheric concentrations of sulfur dioxide, *J. Atmos. Chem.*, *13*, 325-342, 1991.

Knoll, G.F., *Radiation Detection and Measurement*, 816 pp., John Wiley, New York, 1979.

Langford, A.O., and F.C. Fehsenfeld, Natural vegetation as a source or sink for atmospheric ammonia: A case study, *Science*, *255*, 581-583, 1992.

Langford, A.O., F.C. Fehsenfeld, J. Zachariassen, and D.S. Schimel, Gaseous ammonia fluxes and background concentrations in terrestrial ecosystems of the United States, *Global Biogeochem. Cycles*, *6*, 459-483, 1992.

Lefer, B.L., The chemistry and dry deposition of atmospheric nitrogen at a rural site in the northeastern United States, Ph.D. thesis, 119 pp., Univ. of N.H., Durham, December 1997.

Lefer, B.L., et al., Enhancement of acidic gases in biomass-burning impacted air masses over Canada, *J. Geophys. Res.*, *99*, 1721-1738, 1994.

Lewin, E.E., R.G. DePena, and J.P. Shimshock, Atmospheric gas and particle measurements at a rural northeastern U. S. site, *Atmos. Environ.*, *20*, 59-70, 1986.

Marti, J.J., A. Jefferson, X.P. Cai, C. Richert, P.H. McMurry, and F. Eisle, $H_2SO_4$ vapor pressure of sulfuric acid and ammonium sulfate solutions, *J. Geophys. Res.*, *102*, 3725-3735, 1997.

Meyers, T.P., B.J. Huebert, and B.B. Hicks, $HNO_3$ deposition to a deciduous forest, *Boundary Layer Meteorol.*, *49*, 395-410, 1989.

Meyers, T.P., B.B. Hicks, R.P.J. Hosker, J.D. Womack, and L.C. Satterfield, Dry deposition inferential measurement techniques--II. Seasonal and annual deposition rates of sulfur and nitrate, *Atmos. Environ.*, *25A* (10), 2361-2370, 1991.

Moody, J.L., J.W. Munger, A.H. Goldstein, D.J. Jacob, and S.C. Wofsy, Harvard Forest regional-scale air mass composition by Patterns in Atmospheric Transport History (PATH), *J. Geophys. Res.*, *103*, 13,181-13,194, 1998.

Moore, K.W., D.R. Fitzjarrald, R.K. Sakai, M.L. Goulden, J.W. Munger, and S.C. Wofsy, Seasonal variation in radiative and turbulent exchange at a deciduous forest in central Massachusetts, *J. Appl. Meteorol.*, *35*, 122-134, 1996.

Munger, J.W., S.C. Wofsy, P.S. Bakwin, S.-M. Fan, M.L. Goulden, B.C. Daube, and A.H. Goldstein, Atmospheric deposition of reactive nitrogen oxides and ozone in a temperate deciduous forest and a subarctic woodland; 1, Measurements and mechanisms, *J. Geophys. Res.*, *101*, 12,639-12,657, 1996.

Munger, J.W., S.-M. Fan, P.S. Bakwin, M.L. Goulden, A.H. Goldstein, A.S. Colman, and S.C. Wofsy, Regional budgets for nitrogen oxides from continental sources: variations of rates for oxidation and deposition with season and distance from source regions, *J. Geophys. Res.*, *103*, 8355-8368 1998.

National Atmospheric Deposition Program, (NRSP-3)/National Trends Network, NADP/NTN Coord. Off., Nat. Resour. Ecol. Lab., Colorado State Univ., Fort Collins, February 17, 1997.

Ollinger, S.V., J.D. Aber, G.M. Lovett, S.E. Millham, R.G. Lathrop, and J.M. Ellis, A spatial model of atmospheric deposition for the northeastern U.S., *Ecol. Appl.*, *3* (3), 459-472, 1993.

Parrish, D.D., R.B. Norton, M.J. Bollinger, S.C. Liu, P.C. Murphy, D.L. Albritton, F.C. Fehsenfeld, and B.J. Huebert, Measurements of $HNO_3$ and $NO_3^-$ particulates at a rural site in the Colorado mountains, *J. Geophys. Res.*, *91*, 5379-5393, 1986.

Parrish, D.D., M. Trainer, M.P. Buhr, B.A. Watkins, and F.C. Fehsenfeld, Carbon monoxide concentrations and their relation to concentrations of total reactive oxidized nitrogen at two rural U.S. sites, *J. Geophys. Res.*, *96*, 9309-9320, 1991.

Parrish, D.D., et al., The total reactive oxidized nitrogen levels and the partitioning between the individual species at six rural sites in eastern North America, *J. Geophys. Res.*, *98*, 2927-2939, 1993.

Peake, E., M.A. MacLean, and H.S. Sandhu, Total inorganic nitrate (particulate nitrate and nitric acid) observations in Calgary, Alberta, *J. Air Pollut. Control Assoc.*, *35*, 250-253, 1985.

Peterson, B.J., and J.M. Melillo, The potential storage of carbon caused by eutrophication of the biosphere, *Tellus*, *37B*, 117-127, 1985.

Richards, L.W., Comments on the oxidation of $NO_2$ to nitrate: Day and night, *Atmos. Environ.*, *17*, 397-402, 1983.

Savoie, D.L., and J.M. Prospero, Particle size distribution of nitrate and sulfate in the marine atmosphere, *Geophys. Res. Lett.*, *9*, 1207-1210, 1982.

Schell, R.W., A historical perspective of atmospheric chemicals deposited on a mountain top peat bog in Pennsylvania, *Int. J. Coal Geol.*, *8*, 147-173, 1987.

Schindler, D.W., and S.E. Bayley, The biosphere as an increasing sink for atmospheric carbon: Estimates from increased nitrogen deposition, *Global Biogeochem. Cycles*, *7*, 717-734, 1993.

Schlesinger, W.H., and A.E. Hartley, A global budget for atmospheric $NH_3$, *Biogeochemistry*, *15*, 191-211, 1992.

Spicer, C.W., J.E. Howes, T.A. Bishop, L.H. Arnold, and R.K. Stevens, Nitric acid measurement methods: An intercomparison, *Atmos. Environ.*, *16*, 1487-1500, 1982.

Stecher, H.A. III, et al., Results of the Gas-Phase Sulfur Intercomparison Experiment (GASIE): Overview of experimental setup, results and general conclusions, *J. Geophys. Res.*, *102*, 16,219-16,236, 1997.

Stelson, A.W., and J.H. Seinfeld, Relative humidity and temperature dependence of the ammonium nitrate dissociation constant, *Atmos. Environ.*, *16*, 983-992, 1982.

Talbot, R.W., A.S. Vijgen, and R.C. Harriss, Measuring tropospheric $HNO_3$: Problems and prospects for nylon filter and mist chamber techniques, *J. Geophys. Res.*, *95*, 7553-7561, 1990.

Talbot, R.W., A.S. Vijgen, and R.C. Harriss, Soluble species in the Arctic summer troposphere: acidic gases, aerosols, and precipitation, *J. Geophys. Res.*, 97, 16,531-16,545, 1992.

Talbot, R.W., et al., Large-scale distributions of tropospheric nitric, formic, and acetic acids over the western Pacific basin during wintertime, *J. Geophys. Res.*, *102*, 28,303-28,313, 1997.

Tang, I.N., On the equilibrium partial pressures of nitric acid and ammonia in the atmosphere, *Atmos. Environ.*, *14*, 819-828, 1980.

Tjepkema, J.D., R.C. Cartica, and H.F. Hemond, Atmospheric concentration of ammonia in Massachusetts and deposition on vegetation, *Nature*, *249*, 445-446, 1981.

Trainer, M., et al., Observations and modeling of the reactive nitrogen photochemistry at a rural site, *J. Geophys. Res.*, *96*, 3045-3063, 1991.

Williams, E.J., et al., An intercomparison of five ammonia measurement techniques, *J. Geophys. Res.*, *97*, 11,591-11,611, 1992.

Wofsy, S.C., M.L. Goulden, J.W. Munger, S.-M. Fan, P.S. Bakwin, B.C. Daube, S.L. Bassow, and F.A. Bazzaz, Net exchange of $CO_2$ in a mid-latitude forest, *Science*, *260*, 1314-1317, 1993.

Wolff, G.T., On the nature of nitrate in coarse continental aerosols, *Atmos. Environ.*, *18*, 977-981, 1984.

Wyers, G.P., R.P. Otjes, and J. Slanina, A continuous-flow denuder for the measurement of ambient concentrations and surface-exchange fluxes of ammonia, *Atmos. Environ.*, *27A*, 2085-2090, 1993.

---

B. Lefer, Advanced Study Program, National Center for Atmospheric Research, 1850 Table Mesa Drive, Boulder, CO 80303. (e-mail: lefer@ucar.edu)

R. Talbot, Institute for the Study of Earth, Oceans, and Space and Earth Sciences Department, Global Atmospheric Chemistry Group, Morse Hall, University of New Hampshire, Durham, NH 03824.

J.W. Munger, Division of Applied Sciences and Department of Earth and Planetary Sciences, Harvard University, 401 ESL, 40 Oxford Street, Cambridge, MA 02138.

(Received February 23, 1998; revised August 6, 1998;
accepted September 11, 1998.)